Liquid Crystals
Publication details, including instructions for authors and subscription information:
http://www.informaworld.com/smpp/title~content=t713926090

Patterned retarders prepared by photoisomerization and photopolymerization of liquid crystalline films

B. M. I. van der Zande[a]; J. Lub[a]; H. J. Verhoef[b]; W. P. M. Nijssen[a]; S. A. Lakehal[a]
[a] Philips Research Laboratories, 5656 AE Eindhoven, The Netherlands [b] Syncom B.V. Kadijk 3, 9747 AT Groningen, The Netherlands

To cite this Article van der Zande, B. M. I. , Lub, J. , Verhoef, H. J. , Nijssen, W. P. M. and Lakehal, S. A.(2006) 'Patterned retarders prepared by photoisomerization and photopolymerization of liquid crystalline films', Liquid Crystals, 33: 6, 723 — 737
To link to this Article: DOI: 10.1080/02678290600647345
URL: http://dx.doi.org/10.1080/02678290600647345

Liquid Crystals, Vol. 33, No. 6, June 2006, 723–737

Patterned retarders prepared by photoisomerization and photopolymerization of liquid crystalline films

B.M.I. VAN DER ZANDE†, J. LUB*†, H.J. VERHOEF‡, W.P.M. NIJSSEN† and S.A. LAKEHAL†

†Philips Research Laboratories, HTC 4, 5656 AE Eindhoven, The Netherlands
‡Syncom B.V. Kadijk 3, 9747 AT Groningen, The Netherlands

(*Received 8 November 2005; accepted 19 January 2006*)

Isomerizable diacrylates derived from cinnamic acid are designed, synthesized and mixed with liquid crystalline diacrylates with the aim of making films with alternating birefringent and isotropic domains by applying the *E–Z* isomerization process at room temperature. The effects of the structure of the isomerizable-mesogenic group on the isotropization efficacy, the efficiency of the *E–Z* isomerization reaction, and film formation are discussed. Compounds derived from cyclohexyl cinnamate are proved to be good candidates that meet a whole set of parameters related to processing and application. These compounds exhibit a low nematic-to-isotropic transition temperature. In addition, they show no yellowing upon irradiation, unlike similar compounds derived from phenyl cinnamate. To elucidate the origin of isotropization of the film by irradiation, the pure *Z*-isomer is prepared by photolysis of the *E*-isomer and subsequent chromatographic separation of both isomers. Analysis of reference samples containing the pure isomers reveals that the decrease in transition temperature can be attributed exclusively to the *E–Z* photoisomerization process. Finally, thin films with alternating birefringent and isotropic parts of $100 \times 100\,\mu m^2$ are obtained by using a combination of photoisomerization in air and photopolymerization in a nitrogen atmosphere, which is referred to as photo-patterning.

1. Introduction

The demands on liquid crystal displays (LCDs) for mobile applications (e.g. phones) have increased over the years, especially for displaying images and video information. For these purposes a better front-of-screen performance will be required from displays, such as wide viewing angle, brightness, good contrast and colour purity. Simultaneously, customers are demanding improved robustness, as well as a reduction in weight and thickness. The most attractive display principle for mobile applications is the transflective LCD because excellent visibility in all lighting conditions is achievable through the balanced combination of backlighting and reflection of the ambient light. To ensure proper optical functioning, these displays need retarder foils. Conventional systems contain a laminated birefringent foil bonded to the polarizer as retardation film. Current state-of-the-art retardation foils are formed by carefully stretching extruded plastic sheets to a fixed retardation value. As a result, the front-of-screen performance cannot be optimized for both the transmissive and reflective modes, forcing a compromise between contrast and viewing angle or contrast and brightness [1, 2]. In order to improve on the front-of-screen performance, and simultaneously on the reduction of thickness, weight and costs, subpixelated micrometer-thin film retarder foils can be created. These foils exhibit different retardation values for the reflective and transmissive subpixels and have to be positioned inside the liquid crystalline cell without causing parallax problems. Figure 1 shows a preferred design of a transflective LCD employing a patterned

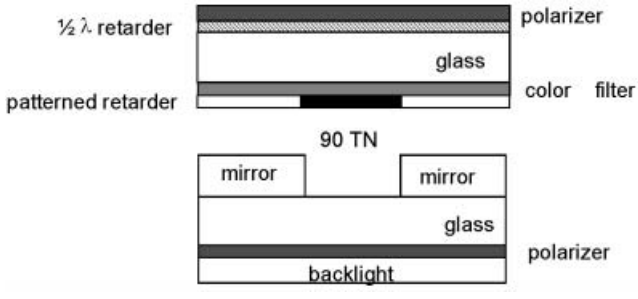

Figure 1. Schematic representation of one pixel of a transflective LCD with patterned retarder (white part ¼ wave plate, black part isotropic).

*Corresponding author. Email: johan.lub@philips.com

Liquid Crystals
ISSN 0267-8292 print/ISSN 1366-5855 online © 2006 Taylor & Francis
http://www.tandf.co.uk/journals
DOI: 10.1080/02678290600647345

thin film retarder. The retardation for the reflective and transmissive mode is ¼ λ and 0 λ, respectively [2, 3].

Various technologies exist to obtain micrometer-thin *uniaxial retardation* films using wet coating techniques combined with photochemistry. Schadt *et al.* [4] reported the fabrication of compensation foils by spin-coating either liquid crystalline polymers or liquid crystalline monomers on top of a photoaligned surface. Photo-orientation phenomena [5, 6] in films of photosensitive azobenzene-containing homopolymers and copolymers can also lead to thin birefringent films that may serve as retardation films. We use the LC-network technology, i.e. *in situ* photopolymerization of liquid crystalline diacrylates [7] to obtain micrometer-thin uniaxial retardation films. In this technology a mixture of liquid crystalline diacrylates doped with photoinitiator is spin-coated on top of a glass plate with an alignment layer. The liquid crystalline diacrylates align themselves on the alignment layer, and the achieved molecular order can be frozen in by photopolymerization of the acrylate groups on UV exposure. The thickness of these films is controlled by the spin-coat conditions and by the concentration of the solution.

The extent to which the film retards polarized light depends on the birefringence (Δn), the film thickness (d), and the angle between the optical axis of the film and the original polarization direction of the light (θ). Therefore, technologies available for creating *alternating retardation* values in micrometer thin retardation films made according to the LC-network technology include director patterning (θ) [4, 8], thickness (d) variations [8, 9] or variations in birefringence (Δn) [10]. For the fabrication of patterned thin film retarders applied in the transflective LCD design given in figure 1, birefringence patterning is preferred to director and thickness patterning because the optical characteristics of an isotropic domain are viewing angle-independent, and surface flatness is required for the assembly and optimal front-of-screen performance of the final LCD. The birefringence of a wet film of liquid crystalline diacrylate monomers can be changed with temperature. Above the nematic-to-isotropic transition the material becomes isotropic, i.e. $\Delta n=0$, and the film becomes optically inactive. Combination of this phase transition with *in situ* photopolymerization results in a patterned thin film retarder [10, 11]. This is achieved by conducting in succession a mask exposure to crosslink the film locally in its nematic state and a flood exposure at a temperature exceeding the nematic-to-isotropic (N-I) transition temperature of the liquid crystalline monomers to fix the remaining isotropic areas.

However, the heating step to isotropize may be undesirable in mass production. It would, therefore, be interesting to apply photoisomerization instead of heating to decrease the birefringence. During the exposure, the properties of a liquid crystalline phase are altered by *E–Z* photoisomerization of compounds containing an olefinic moiety, such as derivatives of stilbene or cinnamic acid. Such an *E–Z* isomerization process has successfully been applied in the manufacturing of cholesteric colour filters [12, 13]. In this process the isomerizable compound also comprises a chiral moiety and the isomerized species exhibits a lower helical twisting power than the original species, resulting in an increase in the reflection wavelength of the cholesteric layer. In the case of the retarders, it is expected that *E–Z* isomerization will lead to a decrease of the N-I transition temperature due to the non-mesogenic character of the *Z*-isomer (bent structure) compared with that of the *E*-isomer (calamitic structure). For this purpose photoisomerizable and photopolymerizable compounds have been designed and synthesized. The search for suitable photoisomerizable and photopolymerizable compounds started by modifying nematic diacrylate **2** (see table 1) which was used as one of the nematic host materials in the cholesteric colour filter manufacturing and in the above-mentioned thermal patterning process. The compounds should accommodate processability at room temperature, the photo-reaction must form clean isomerization products, and the monomers need to exhibit a nematic phase at room temperature. Moreover, the polymerized film has to be thermally stable because several high temperature steps, such as indium tin oxide sputtering and polyimide baking, are involved in the LCD manufacturing process. This paper describes the synthesis, photochemistry and film formation of newly designed photoisomerizable diacrylates that fulfill all these conditions. In addition, the mechanism behind isotropization of aligned monomers in their nematic phase is elucidated and patterning with a resolution of about 100 µm is demonstrated.

2. Experimental

2.1. *Materials*

Literature procedures were used to obtain 4-(6-acryloyloxyhexyloxy)cinnamic acid (**13**) [14], 4-(6-acryloyloxyhexyloxy)benzoic acid (**10**) [15] and *trans*-4-[6-(tetrahydropyran-2-yloxy)hexyloxy]cyclohexanol (**17**) [16]. [4-(3-Acryloyloxypropyloxy)benzoyloxy]-2-methylphenyl 4-(3-acryloyloxypropyloxy)benzoate (**1**), [4-(3-acryloyloxyhexyloxy)benzoyloxy]-2-methylphenyl 4-(3-acryloyloxyhexyloxy)benzoate (**2**) and

Table 1. Structures and thermal properties of nematic liquid crystalline diacrylates **1** and **2** and of the photoisomerizable diacrylates described in this paper.

Compound number	Structure	Transition temperatures/°C
1	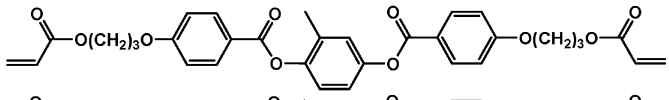	Cr–73–N–129–I
2	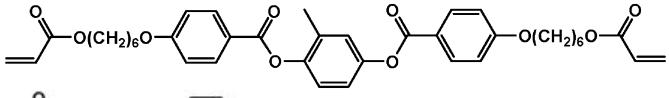	Cr–86–N–116–I
3	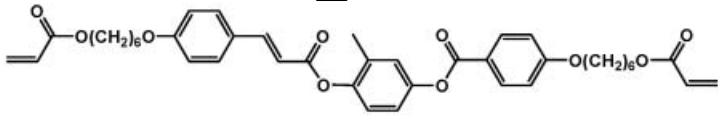	Cr–50–N–149–I
4	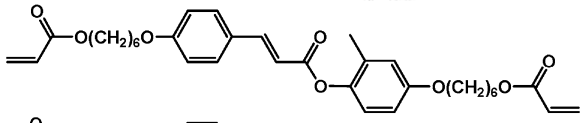	(N–41–I) Cr–52–I
5	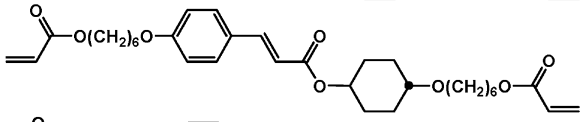	Cr–54–I
6	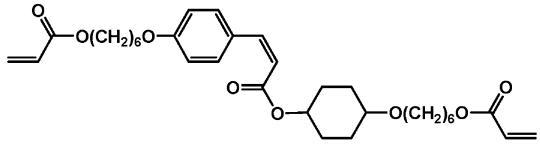	oil

RM522 were obtained from Merck. The photoinitiator, Irgacure 651, was obtained from Ciba Specialty Chemicals. All other chemicals were obtained from Aldrich.

2.2. *Synthesis*

The synthesis routes to compounds **3**, **4**, **5** and **6** are summarized in schemes 1–3.

2.2.1. Synthesis of 4-acetyloxy-2-methylphenol (7). 100 ml of acetic anhydride (1.0 mol) was added dropwise to a stirred solution of 124 g of methylhydroquinone (1.0 mol) and 40 g of sodium hydroxide (1.0 mol) in 100 ml of water to which 300 g of ice was added. Once the mixture had become neutral, 300 ml of dichloromethane was added. After separation, the organic layer was extracted with 200 ml of water, twice with 200 ml of 5% aqueous sodium bicarbonate and once with 200 ml of aqueous sodium chloride. The solid obtained after drying over magnesium sulphate and evaporation was crystallized twice from a 1/1 (wt/wt) mixture of toluene and ligroin. 43.7 g of a light yellow powder (26%) was obtained, m.p. 96°C (lit 92°C [17]). ^{1}H NMR (δ in ppm, relative to TMS, J in Hz): 6.79 (d, 1H, J=3.0, H^b), 6.71 (dd, 1H, J_1=8.7, J_2=3.0, H^c), 6.59 (d, 1H, J=8.7, H^d), 5.53 (s, 1H, H^e), 2.27 (s, 3H, H^a), 2.16 (s, 3H, H^f).

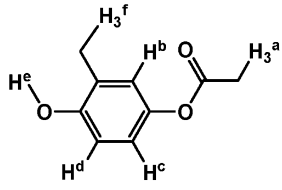

2.2.2. Synthesis of 3-methyl-4-(tetrahydropyranyl-2-yloxy)phenol (9). 35 ml (0.38 mol) of dihydropyran was added dropwise to a solution of 43 g of 4-acetyloxy-2-methylphenol (**7**) (0.26 mol) and 2 g of 4-toluenesulphonic acid (0.01 mol) in 200 ml of diethyl ether. After stirring for 2 h at room temperature, the solution was extracted twice with 100 ml of 10% aqueous sodium hydroxide and once with 200 ml brine. After evaporation, the intermediate 3-methyl-4-(tetrahydropyranyl-2-yloxy)phenyl acetate (**8**) was obtained as a brown liquid. This liquid was mixed with 40 g of sodium hydroxide (1.0 mol), 200 ml of water and 1 g of sodium bisulphite. The mixture was heated under reflux under a nitrogen atmosphere until it became clear. After extraction with 100 ml of diethyl

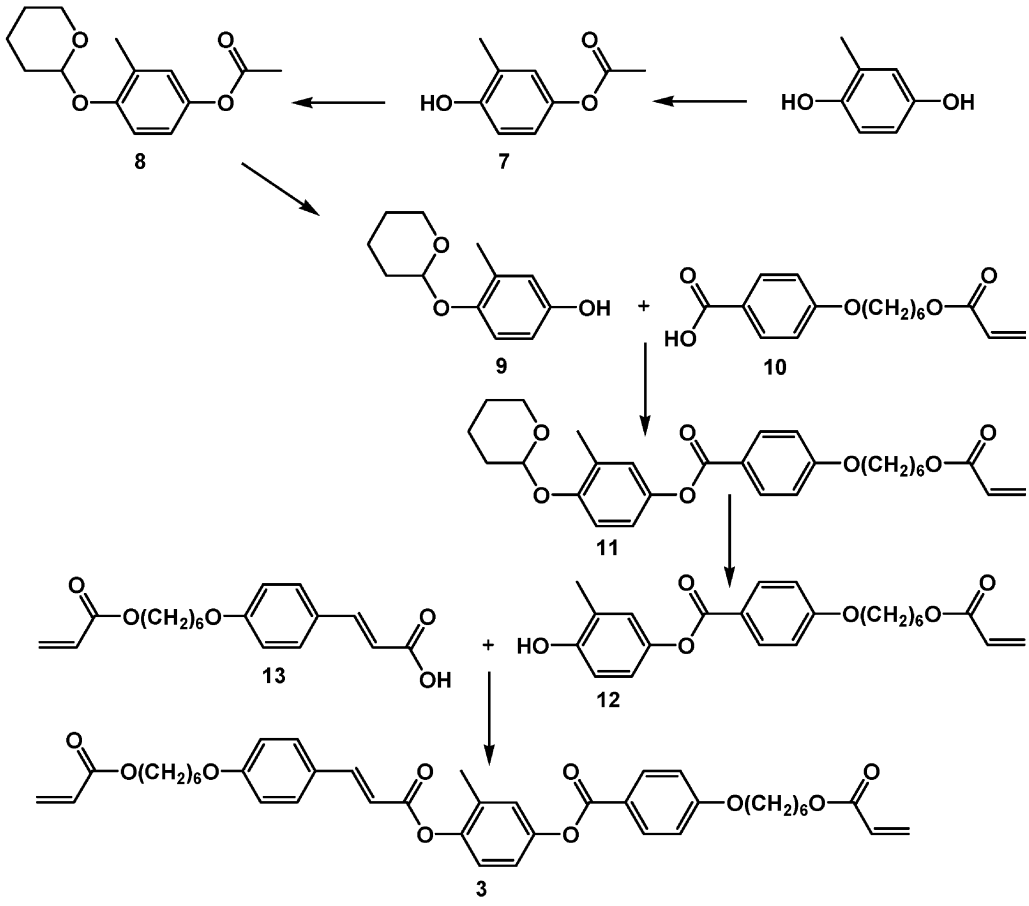

Scheme 1. Synthesis of compound **3**.

ether, a 2.5M HCl solution was added until pH=7, upon which a white precipitate appeared that was filtered off and washed with 300 ml of water; 41.7 g (77 %) of a white powder was obtained.

2.2.3. Synthesis of 4-hydroxy-3-methylphenyl 4-(6-acryloyloxyhexyloxy)benzoate (12). 6.2 g (0.03 mol) of *N*,*N*′-dicyclohexylcarbodiimide (DCC) was added, whilst stirring, to a mixture of 8.8 g (0.03 mol) of compound **10**, 6.3 g (0.03 mol) of compound **9**, 0.37 g (3 mmol) of 4-*N*,*N*-dimethylaminopyridine (DMAP) and 50 ml of dichloromethane in an ice bath. After stirring for one night at room temperature, the mixture was filtered over 15 g of silica and the solvent allowed to evaporate to leave the intermediate 4-(tetrahydropyran-2-yloxy)-3-methylphenyl 4-(6-acryloyloxyhexyloxy)benzoate (**11**) as a clear oil that solidified on standing. This intermediate was mixed with 0.38 g of pyridinium 4-toluenesulphonate (1.5 mmol) and 50 ml of ethanol. After the mixture had been heated for 4 h at 55°C, a clear solution was obtained. After the addition of 30 ml water, 10.7 g (94% yield) of the product crystallized on cooling.

2.2.4. Synthesis of 4-(6-acryloyloxyhexyloxy)benzoyloxy-2-methylphenyl 4-(6-acryloyloxyhexyloxy)cinnamate (3). 4.1 g (0.02 mol) of DCC was added, whilst stirring, to a mixture of 8.0 g (0.02 mol) of compound **12**, 6.4 g (0.02 mol) of compound **13**, 0.25 g (2 mmol) of DMAP and 80 ml of dichloromethane in an ice/water bath. After stirring for one night at room temperature, the solvent was evaporated; 12.2 g (87%) of the product was obtained after recrystallization from ethanol. ^{1}H NMR (δ in ppm, relative to TMS, J in Hz): 8.13 (d, 2H, J=9.0, H^r), 7.84 (d, 1H, J=16.2, H^l), 7.54 (d, 2H, J=8.7, H^k), 7.13 (d, 1H, J=8.7, H^p), 7.12 (d, 1H, J=3.0, H°), 7.06 (dd, 1H, J_1=8.7, J_2=3.0, H^q), 6.96 (d, 2H, J=9.0, H^s), 6.92 (d, 2H, J=8.7, H^j), 6.53 (d, 1H, J=16.2, H^m), 6.41 (dd, 2H, J_1=17.3, J_2=1.5, H^a), 6.13 (dd, 2H, J_1=17.3, J_2=10.5, H^c), 5.82 (dd, 2H, J_1=10.5, J_2=1.5, H^b), 4.17 (t, 4H, J=6.4, H^d), 4.05 (t, 2H, J=6.4, H^t), 4.00 (t, 2H, J=6.4, H^i), 2.24 (s, 3H, H^n), 1.83 (m, 4H, H^h), 1.72 (m, 4H, H^e), 1.50 (m, 8H, H^f+H^g).

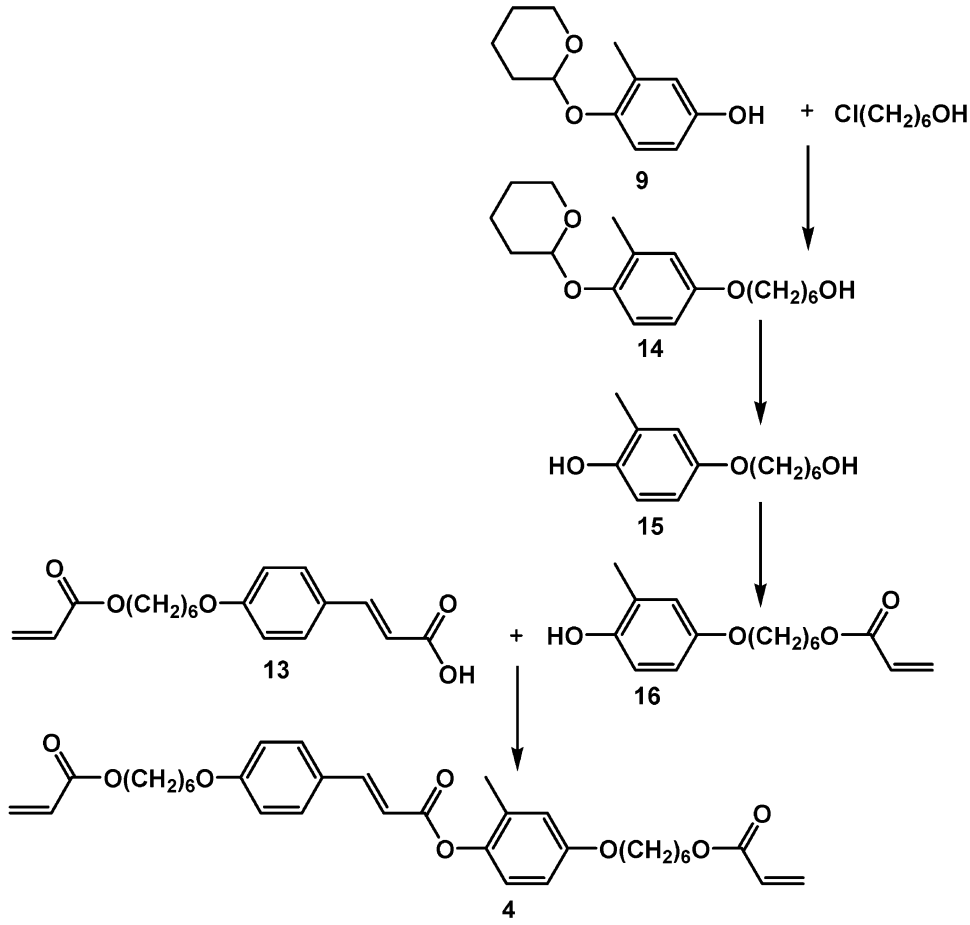

Scheme 2. Synthesis of compound **4**.

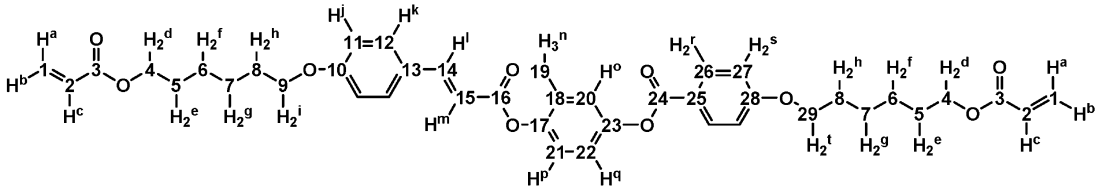

^{13}C NMR (δ in ppm, relative to TMS): 166.7 (C^3), 165.8 (C^{24}), 165.3 (C^{16}), 163.8 (C^{28}), 161.7 (C^{10}), 148.8 (C^{23}), 147.3 (C^{17}), 146.9 (C^{14}), 132.7 (C^{26}) 132.1 (C^{18}), 131.0 (C^1), 130.4 (C^{12}), 129.0 (C^2), 127.1 (C^{13}), 124.5 (C^{20}), 123.2 (C^{21}), 122.0 (C^{25}), 120.4 (C^{22}), 115.3 (C^{11}), 114.7 (C^{27}) 114.5 (C^{15}), 68.5 (C^{29}), 68.4 (C^9), 64.9 (C^4), 29.4 (C^8), 28.9 (C^5), 26.1 (C^6+C^7), 16.8 (C^{19}).

2.2.5. Synthesis of 4-(6-hydroxyhexyloxy)-2-methylphenol (15). A mixture of 2.0 g (0.05 mol) of sodium hydroxide, 10.4 g (0.05 mol) of compound **9**, 1.0 g of sodium iodide, 7.2 g (0.05 mol) of chlorohexanol and 50 ml of ethanol was heated under reflux for 16 h. After evaporation of the ethanol, 50 ml of diethyl ether was added and the organic layer was extracted twice with 60 ml of 5% aqueous sodium hydroxide and then with 50 ml of saturated aqueous sodium chloride. After evaporation of the diethyl ether, intermediate **14** was obtained which was dissolved in 25 ml of ethanol that contained 0.5 ml concentrated HCL. After 30 min stirring, 3 ml of 10% aqueous sodium hydroxide was added and the solvent was evaporated. The remaining product was dissolved in 50 ml of 5% NaOH. After two

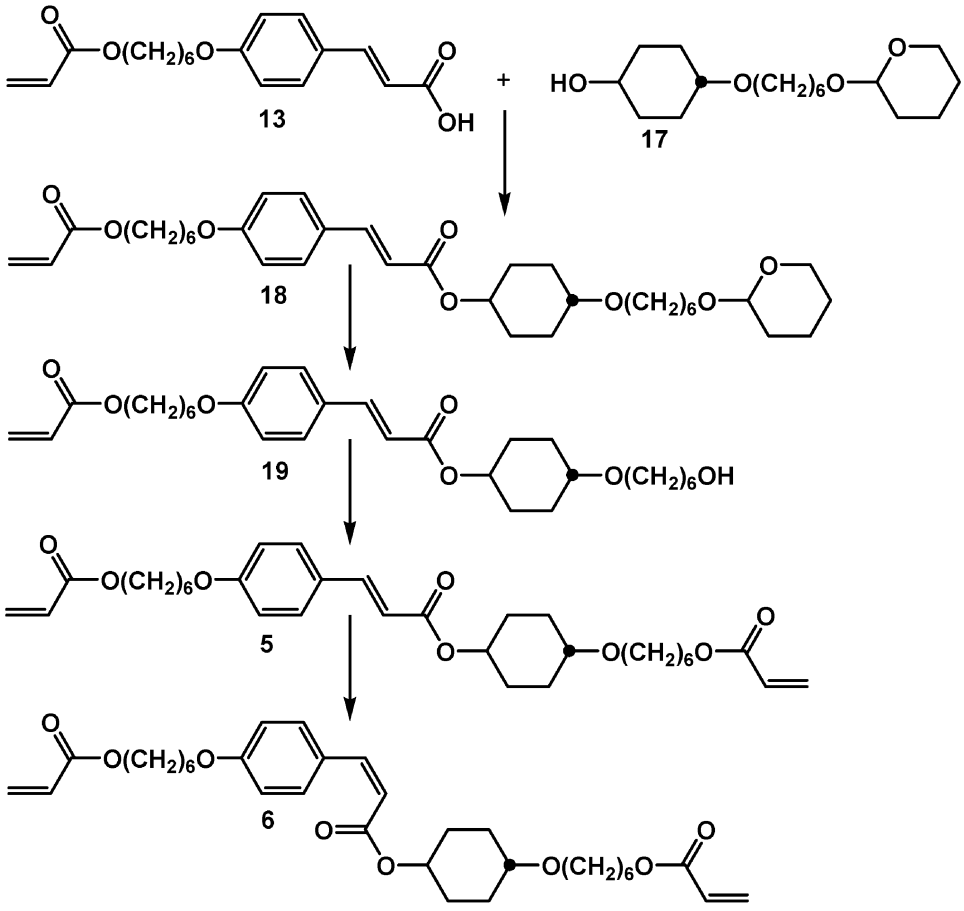

Scheme 3. Synthesis of compounds **5** and **6**.

extractions with 40 ml of diethyl ether, the aqueous layer was acidified with 7 ml of concentrated HCL while being stirred in an ice/water bath. The oil that separated was extracted twice with 40 ml of diethyl ether; 6.2 g (56%) of the product was obtained as an oil after drying over magnesium sulphate and evaporating the solvent.

2.2.6. Synthesis of 4-(6-acryloyloxyhexyloxy)-2-methylphenol (16). 2.8 g (30 mmol) of acryloyl chloride was added dropwise to a solution of 6.2 g (28 mmol) of compound **15** and 3.7 g (30 mmol) of N,N-dimethylaniline in 30 ml of dry dichloromethane, while being cooled in an ice/water bath. After 16 h stirring at room temperature, the solvent was evaporated. The remaining oil was dissolved in 50 ml of diethyl ether and then extracted twice with 30 ml of 2N HCL and with 50 ml saturated aqueous NaCl. 6.3 g (83%) of the product was obtained as an oil that solidified on standing, after drying over $MgSO_4$ followed by evaporation of diethyl ether.

2.2.7. Synthesis of 4-(6-acryloyloxyhexyloxy)-2-methylphenyl 4-(6-acryloyloxyhexyloxy)cinnamate (4). 4.13 g (0.02 mol) of DCC was added to a mixture of 5.6 g (0.02 mol) of compound **16**, 6.4 g (0.02 mol) of compound **13**, 0.25 g (2.0 mmol) of DMAP and 80 ml of dichloromethane while cooling in an ice/water bath. After stirring for 16 h at room temperature, the mixture was filtered over 12 g of silica and the solvent allowed to evaporate; 9.6 g (83%) of the product was obtained as a white powder after recrystallization from ethanol at 5°C. ^{1}H NMR (δ in ppm, relative to TMS, J in Hz): 7.82 (d, 1H, J=16.2, H^l), 7.53 (d, 2H, J=8.7, H^k), 6.97 (d, 1H, J=3.0, H°), 6.91 (d, 2H, J=8.7, H^j), 6.77 (d, 1H, J=8.7, H^p), 6.50 (d, 1H, J=16.2, H^m), 6.73 (dd, 1H, J_1=8.7, J_2=3.0, H^q), 6.41 (dd, 2H, J_1=17.3, J_2=1.5, H^a), 6.13 (dd, 2H, J_1=17.3, J_2=10.5, H^c), 5.82 (dd, 2H, J_1=10.5, J_2=1.5, H^b), 4.17 (t, 4H, J=6.4, H^d+H^w), 4.00 (t, 2H, J=6.4, H^i), 3.94 (t, 2H, J=6.4, H^r), 2.18 (s, 3H, H^n), 1.80 (m, 4H, H^h+H^s), 1.72 (m, 4H, H^e+H^v), 1.60–135 (m, 8H, H^f+H^g+H^t+H^u).

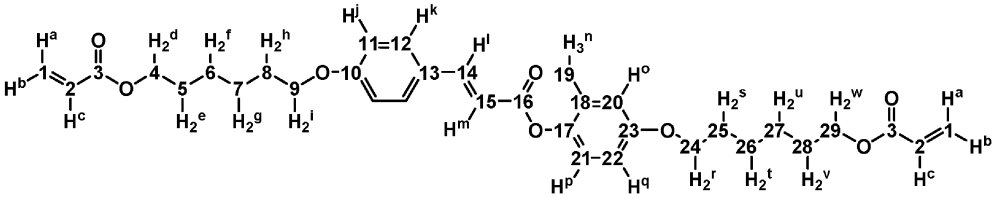

^{13}C NMR (δ in ppm, relative to TMS): 166.7 (C^{3}), 166.3 (C^{16}), 161.6 (C^{10}), 157.1 (C^{23}), 146.5 (C^{14}), 143.4 (C^{17}), 131.7 (C^{18}), 131.0 (C^{1}), 130.4 (C^{12}), 129.0 (C^{2}), 127.2 (C^{13}), 122.9 (C^{21}), 117.2 (C^{20}), 115.3 (C^{11}), 114.8 (C^{15}), 112.8 (C^{22}), 68.4 (C^{9}+C^{24}), 64.9 ($C^{4+}C^{29}$), 29.6 (C^{25}), 29.4 (C^{8}), 28.9 ($C^{5+}C^{28}$), 26.1 (C^{6}+C^{7}+C^{26}+C^{27}), 16.9 (C^{19}).

2.2.8. Synthesis of trans-4-(6-hydroxyhexyloxy)cyclohexyl 4-(6-acryloyloxyhexyloxy)cinnamate (19). 1.5 g (7.5 mmol) of DCC was added to a mixture of 2.3 g (7.5 mmol) of compound **17**, 2.4 g of compound **13** (7.5 mmol), 0.12 g (0.8 mmol) of DMAP and 40 ml of dichloromethane while stirring in an ice bath. After stirring overnight at room temperature, the reaction mixture was filtered through 4 g of silica and the solvent was allowed to evaporate. The crude intermediate *trans*-4-[-6-(tetrahydropyran-2-yloxy)hexyloxy]cyclohexyl 4-(6-acryloyloxyhexyloxy)cinnamate (**18**) was dissolved in 25 ml of ethanol to which 0.63 g (2.5 mmol) of pyridinium 4-toluenesulphonate was added. After the solution had been heated for 5 h at 60°C, the ethanol was evaporated; 1.9 g (50%) of the product was obtained after flash chromatography (silica, dichloromethane/ethyl acetate, 90/10 wt/wt).

2.2.9. Synthesis of *trans*-4-(6-acryloyloxyhexyloxy)cyclohexyl 4-(6-acryloyloxyhexyloxy)cinnamate (5). 0.7 ml (8.4 mmol) of acryloylchloride was added to a solution of 1.9 g (3.8 mmol) of compound **19** and 1.1 ml (8.4 mmol) of *N*,*N*-dimethylaniline in 20 ml of dichloromethane, while cooling in an ice bath. After stirring overnight, the solution was extracted with 30 ml of water and 30 ml of 5% aqueous HCl. After drying over $MgSO_4$, the solution was passed through a thin silica layer and the solvent allowed to evaporate; 1.5 g of the product (70%) was obtained as a white powder after crystallization from a 1/3 (wt/wt) water/ethanol mixture. ^{1}H NMR (δ in ppm, relative to TMS, J in Hz): 7.62 (d, 1H, J=16.2, H^{l}), 7.46 (d, 2H, J=8.7, H^{k}), 6.88 (d, 2H, J=8.7, H^{j}), 6.41 (dd, 2H, J_1=17.3, J_2=1.5, H^{a}), 6.29 (d, 1H, J=16.2, H^{m}), 6.13 (dd, 2H, J_1=17.3, J_2=10.5, H^{c}), 5.82 (dd, 2H, J_1=10.5, J_2=1.5, H^{b}), 4.88 (m, 1H, H^{n}), 4.17 (t, 2H, J=6.4, H^{d}), 4.16 (t, 2H, J=6.4, H^{w}), 3.99 (t, 2H, J=6.4, H^{i}), 3.44 (t, 2H, J=6.4, H^{r}), 3.32 (m, 1H, H^{q}), 2.03 (m, 4H, H°+H^{p}), 1.81 (q, 2H, J=6.4, H^{h}), 1.70–135 (m, 20H, H^{e}+H^{f}+H^{g}+$H^{\circ\prime}$+$H^{p\prime}$+H^{s}+H^{t}+H^{u}+H^{v}). ^{13}C NMR (δ in

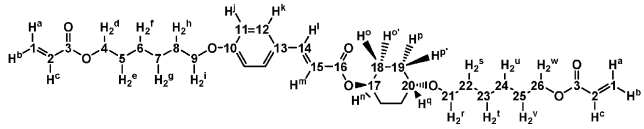

ppm, relative to TMS): 167.2 (C^{16}), 166.7 (C^{3}), 161.2 (C^{10}), 144.6 (C^{14}), 131.0 (C^{1}), 130.0 (C^{12}), 129.0 (C^{2}), 127.4 (C^{13}), 116.4 (C^{15}), 115.2 (C^{11}), 76.4 (C^{20}), 72.1 (C^{17}), 68.6 (C^{21}), 68.3 (C^{9}), 64.9 ($C^{4+}C^{26}$), 30.4 (C^{22}), 29.4 (C^{8}), 29.3 (C^{19}), 29.1 (C^{18}), 29.0+28.9 ($C^{5+}C^{25}$), 26.3+26.2 (C^{23}+C^{24}), 26.1 (C^{6}+C^{7}).

2.2.10. Synthesis of *trans*-4-(6-acryloyloxyhexyloxy)-cyclohexyl (*Z*)-3-[4-(6-acryloyloxyhexyloxy)phenyl]acrylate (6). A solution of 0.5 g of compound **5** in 10 ml of dichloromethane was irradiated with a 350 nm light source (Philips TL-08) for 24 h. After evaporation, the isomers were separated by means of column chromatography (silica/dichloromethane); 140 mg of the product (28%) was obtained as an oil. ^{1}H NMR (δ in ppm, relative to TMS, J in Hz): 7.67 (d, 2H, J=8.7, 6.86 (d, 2H, J=8.7, H^{j}), 6.82 (d, 1H, J=16.2, H^{l}), H^{k}), 6.41 (dd, 2H, J_1=17.3, J_2=1.5, H^{a}), 6.13 (dd, 2H, J_1=17.3, J_2=10.5, H^{c}), 5.82 (dd, 2H, J_1=10.5, J_2=1.5, H^{b}), 5.80 (d, 1H, J=16.2, H^{m}), 4.81 (m, 1H, H^{n}), 4.17 (t, 2H, J=6.4, H^{d}), 4.16 (t, 2H, J=6.4, H^{w}), 3.98 (t, 2H, J=6.4, H^{i}), 3.42 (t, 2H, J=6.4, H^{r}), 3.27 (m, 1H, H^{q}), 1.99 (m, 4H, H°+H^{p}), 1.81 (q, 2H, J=6.4, H^{h}), 1.70–135 (m, 20H, H^{e}+H^{f}+H^{g}+$H^{\circ\prime}$+$H^{p\prime}$+H^{s}+H^{t}+H^{u}+H^{v}).

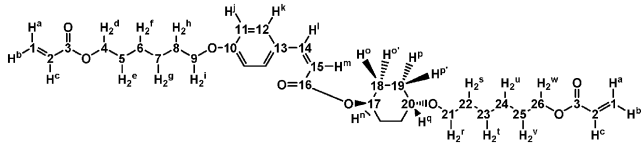

^{13}C NMR (δ in ppm, relative to TMS): 166.7 (C^{3}), 164.6 (C^{16}), 160.3 (C^{10}), 143.5 (C^{14}), 132.6 (C^{1}), 130.0 (C^{12}), 129.0 (C^{2}), 127.7 (C^{13}), 117.9 (C^{15}), 115.2 (C^{11}), 76.4 (C^{20}), 72.2 (C^{17}), 68.6 (C^{21}), 68.2 (C^{9}), 64.9

($C^{4+}C^{26}$), 30.4 (C^{22}), 29.5 (C^{8}), 29.3 (C^{19}), 29.1 (C^{18}), 29.0+28.9 ($C^{5+}C^{25}$), 26.3+26.2 ($C^{23}+C^{24}$), 26.1 ($C^{6}+C^{7}$).

2.3. *Film formation*

A solution was prepared by dissolving 0.5 g of **1**, 0.5 g of the newly designed molecule **3, 4** or **5**, 0.01 g of Irgacure 651 and 0.01 g of RM522 in 2 g of xylene at 70°C. This solution was spin-coated on a substrate with rubbed polyimide (AL 1051) as the alignment layer. The spin conditions of the Convac Spinner were 60 s at 1500 rpm, yielding a birefringent film with a thickness of about 1.7 μm. The rubbed polyimide established nearly planar alignment of the LC monomers in their nematic phase with the director parallel to the rubbing direction. The formation of a monodomain was facilitated by an annealing step on a hot plate at 55°C for 60 s.

In order to introduce the intended *E–Z* isomerization, the annealed film was exposed in air using a Fairlight exposure machine at UV intensity of $5\,mW\,cm^{-2}$ (313 nm). For the mask exposures required to pattern the thin film, a checkerboard mask with feature sizes of $1\times1\,mm^2$ and $100\times100\,\mu m^2$ was used. Crosslinking of the film was achieved by a flood exposure in nitrogen for 5 min using a Philips HPA lamp ($4\,mW\,cm^{-2}$, 365 nm).

2.4. *Methods*

Absorption UV spectra were recorded in a dilute acetonitrile solution using a Unicam UV2-100 spectrometer. Irradiation of the cuvettes was performed with a TL08 light source (Philips, broadband, $\lambda=350$ nm). NMR spectra were recorded with a Bruker DPX300 spectrometer in deuterated dichloromethane or deuterated chloroform. The ^{1}H and ^{13}C NMR data were fully consistent with the required structures and confirmed the purity of all the final products. Interpretation of the spectra was carried out with the aid of 2D ^{13}C-^{1}H correlation spectra. High performance liquid chromatography (HPLC) was performed on a LiChroCart 250-4; RP-18 (5 mm) Cat. 1.50995 column from Merck. The eluant used was a mixture of water and methanol in the volume percentage ratio 17/83, respectively, with a flow of $1.0\,ml\,min^{-1}$. A volume of 25 ml was pumped into the eluant by a Waters autosampler 717 plus. The detection was performed with a Waters 996 DAD detector at the isosbestic point of the mixture, i.e. 268 nm.

The birefringence of *non-polymerized wet monomeric* films in their nematic phase was measured with a polarizing microscope equipped with an optical compensator (Leitz Tilting Compensator 1942 K) and a Mettler Toledo FP5 hot stage. The sample was placed between crossed polarizers with the orientation axis of the cell at 45° with the crossed polarizers. The optical compensator was placed perpendicular to the orientation axis of the film. The birefringence (Δn) was obtained according to: $\Delta n=R/d$. The retardation (R) of the *polymerized patterned* thin film retarders was measured at 547 nm using an SS547-10 colour filter, a Leica polarized light microscope connected to a Leitz Wetzlar photomultiplier and a Keithley photometer. The sample was placed between polarizers and the orientation axis of the cell formed 45° with the transmissive axis of the analyser. The transmission of light was then measured for both crossed, T_c, and parallel polarizers, T_p, using a pinhole of about $50\times50\,\mu m^2$. From the measured transmissions the retardation, R(nm), was calculated from:

$$R=\arctan\left(\frac{T_c}{T_p}\right)^{\frac{1}{2}}\frac{547}{\pi}.$$

The surface profiles and thicknesses were determined by interferometry performed on a Wyko Interferometer and Tencor surface profiler.

3. Results and discussion

3.1. *Synthesis, photochemistry and film formation of compounds 3 and 4*

For the purpose of local isotropization of a film made from nematic monomers, the photoisomerizable compound **3** that is structurally related to the host **2** was synthesized. One of the benzoate moieties was replaced by an isomerizable cinnamic moiety. The synthetic steps are outlined in scheme 1. The protected intermediate **9** has been used to esterify exclusively the 4-hydroxyl group of methylhydroquinone with acid **10**. As a result, the intermediates **11** and **12** are single isomeric compounds and relatively easy to purify. However, the protected methylhydroquinone **9** could not be made simply by reaction between methylhydroquinone and 3,4-dihydropyran, because this reaction led to a 1:1 mixture of both possible isomers [18]. For that reason **9** has been made using monoacetate **7** that could be isolated from its isomer. The properties of **3** are presented in table 1. The clearing point of **3** is 33°C higher than that of compound **2,** which is attributable to the replacement of the benzoate moiety by the cinnamic moiety. The presence of the methyl group in the middle ring of **3** mediates the suppression of crystallization of this compound in mixtures with nematic diacrylates such as **1**.

To study the film formation and the ability of isotropization, a xylene solution containing the compounds **1** and **3** in a 1:1 weight ratio was spin-coated on glass plates coated with a thin rubbed polyimide layer.

Note that 1 % photoinitiator and 1% surfactant were present in all mixtures used for the film fabrication. However, in the following we do not mention the presence of the photoinitiator and surfactant. In this way a birefringent film of uniaxially- and planarly-aligned monomers in their nematic phase was obtained (i.e. the local directors point in one direction, which is parallel to the substrate). The crystallization was indeed suppressed, allowing for further processing at room temperature. Figure 2 (*a*) shows the relative retardation as a function of the temperature for the non-exposed and UV-exposed film. The relative retardation is the quotient of the retardation measured at an elevated temperature and that measured at 30°C. The exposure

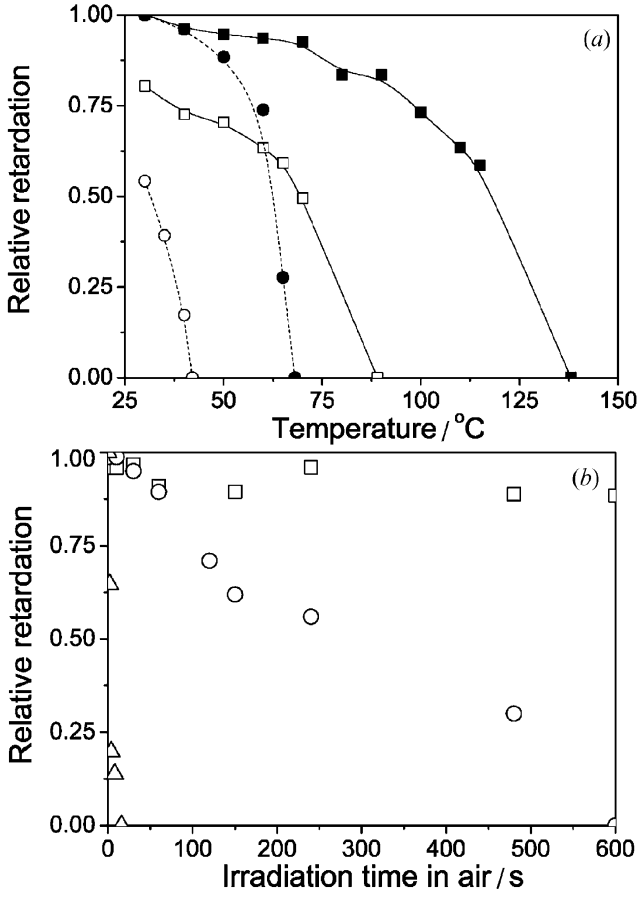

Figure 2. (*a*) The relative retardation of a film made of **3** and **1** in a 1:1 weight ratio before (■) and after 300 s irradiation (□), and of a film made of **4** and **1** in 1:1 weight ratio before (●) and after irradiation (○) as a function of temperature. (*b*) The relative retardation at room temperature of films irradiated for varying times before crosslinking: (□) made of **3** and **1** in a 1:1 weight ratio and (○) made of **4** and **1** in a 1:1 weight ratio. Figure 2 (*b*) includes the relative retardation as a function of irradiation time for films made of **5** and **1** in a 1:1 weight ratio (Δ). The traces in figure 2 (*a*) serve as a 'guide for the eye'.

(5 mW cm^{-2}, 313 nm) was performed for 300 s in air in order to avoid polymerization. The relative retardation for the non-exposed film decreased monotonically as the temperature rose in the nematic phase range and dropped to zero at the transition temperature of 138°C. At temperatures exceeding the nematic-to-isotropic transition of the monomeric mixture, the film became isotropic and consequently non-birefringent. A similar curve was found for the exposed film after irradiation, with the difference that the N-I transition temperature shifted towards a lower temperature, i.e. 89°C. Upon exposure the transition temperature decreased further, e.g. after 600 s the $T_{I\text{-}N}$=76°C, but did not reach room temperature within reasonable exposure times. Hence, a patterned thin film retarder for application in a transflective LCD can be manufactured in the temperature range between 76°C and 138°C because in this temperature range a strong decrease in retardation occurs when the film is UV exposed. However, at room temperature the retardation only dropped slightly. As a consequence, isotropization at room temperature within reasonable irradiation times cannot be achieved. This is demonstrated in figure 2 (*b*). The drop in relative retardation of films that have been photoisomerized and photopolymerized at room temperature is plotted against the irradiation time. The relative retardation of a film made from **1** and **3** in a 1:1 weight ratio (squares) dropped about 15% upon a 600 s exposure in air at room temperature. Apparently, the initial transition temperature of the monomeric film should be lower to allow for a shift beyond room temperature within reasonable exposure times.

To anticipate a lower N-I transition temperature the photoisomerizable and photopolymerizable compound **4** was designed. Compound **4** contains two aromatic rings instead of the three that are present in compound **3**. Its synthesis is outlined in scheme 2. The protected methyl hydroquinone **9** was used again to obtain **4** and the intermediate compounds **14**, **15** and **16** as single isomers. Table 1 shows that this new diacrylate exhibits an isotropic transition at 41°C, more than 100°C lower than compound **3**. The solid circles in figure 2 (*a*) show the dependence of the relative retardation as a function of the temperature of a film spin-coated from a xylene solution containing a mixture of **1** and **4** in a 1:1 weight ratio. The initial N-I transition of a non-exposed film was 68°C. A shift in the transition temperature from 68 to 40°C occurred when the film was UV-exposed in air for 300 s (5 mW cm^{-2}, 313 nm). The birefringent film became completely isotropic near room temperature after irradiation for 600 s. Hence, a patterned thin film retarder can be made at room temperature. Figure 2 (*b*) demonstrates the decrease in relative retardation of a

film made from compounds **1** and **4** that is photoisomerized and photopolymerized at room temperature. Indeed, the film became isotropic after 600 s irradiation.

However, the photoisomerized films of both **3** and **4** became yellow, indicating that another photochemical process was operative in addition to *E–Z* isomerization. This yellowing was clearly apparent from the UV-vis absorption spectra recorded on a diluted solution of **4** in acetonitrile that was incrementally UV exposed. These difference UV-vis absorption spectra (i.e. the non-irradiated spectrum is subtracted from the irradiated one) are presented in figure 3. The absorption in the blue region increases upon irradiation. NMR experiments showed that upon irradiation the signals of the olefinic protons at 7.8 and 6.5 ppm (H_l and H_m, respectively, see experimental) shift to approximately 7.0 and 6.0 ppm, which is typical for *E–Z* isomerization. But, in addition, the NMR spectra contained a large number of unidentifiable peaks after exposure, indicating the occurrence of side reactions. These side reactions are probably attributable to α-splitting of the ester moiety. Aromatic cinnamic esters are known to undergo this α-splitting relatively easily as a first step of the photo-Fries rearrangement. The photo-Fries rearrangement results in compounds that absorb in the blue region of the visible spectrum, thus causing the yellowing appearance of the films [19]. With regard to application in patterned thin film retarders, these side reactions lead to optically imperfect films. Replacement of the aromatic ring that originates from methylhydroquinone (scheme 2) by a cyclohexane ring makes the compound less vulnerable to α-splitting of the ester moiety. An additional advantage of an aliphatic cinnamate is that potential side products lead to compounds that absorb less in the visible region because they miss the aromatic ring. For this reason compound **5** was designed, in which a cyclohexyl ester moiety replaces the aromatic ester moiety of **4**.

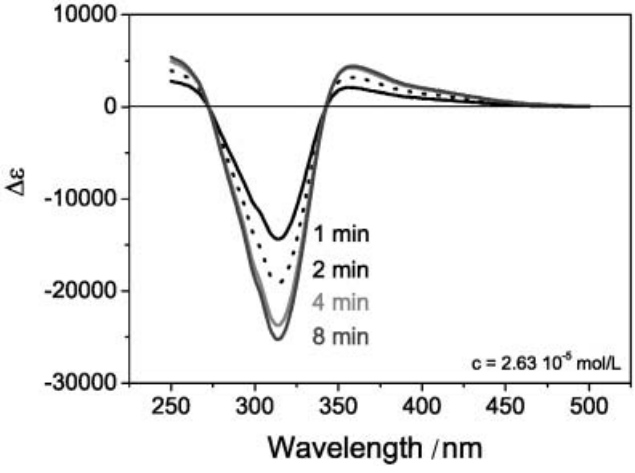

Figure 3. The difference UV-vis absorption spectra (i.e. the non-irradiated spectrum is subtracted from the irradiated one) for various irradiation times of compound **4** in acetonitrile.

3.2. *Synthesis, photochemistry and film formation of compound 5*

The synthesis of the cyclohexane derivative **5** is outlined in scheme 3. It was not possible to make an acrylate-containing cyclohexanol derivative that could be esterified with cinnamic derivative **13** to obtain **5**. Therefore, cyclohexanol derivative **17** was used. This compound has been described previously [16]. Comparison of the thermal data of **4** and **5** (see table 1) reveals that when the cyclohexyl ester moiety replaces the aromatic ester moiety a compound is obtained that is isotropic at room temperature. However, a film of a mixture of **5** and **1** is nematic at room temperature.

The orientation of the monomeric diacrylates in films spin-coated from a xylene solution containing **5** and **1** in a 1:1 weight ratio was uniaxial and planar, similar to the results obtained with compound **4** and nematic diacrylate **1**. The birefringent films enabled processing at room temperature. The initial N-I transition temperature for a non-exposed film was 55°C and shifted to below room temperature after a 16 s UV exposure (5 mW cm^{-2}, 313 nm). Figure 2 (*b*) includes the decrease in relative retardation of films made from compounds **1** and **5** that have been photoisomerized and photopolymerized at room temperature (triangles). An isotropic film has already been obtained after a 16 s UV exposure in air. Hence, the isotropization efficacy is much higher than that of **3** and **4**, which is probably attributable to the low starting N-I transition and the relatively large amount of *Z*-isomer in the photostationary state; i.e. 60% conversion has been observed with NMR (solution in dichloromethane).

In order to find out whether or not the yellowing observed with the all-aromatic compounds **3** and **4** occurs with **5**, a solution of **5** in acetonitrile was irradiated and the UV-vis absorption spectra were recorded. The results are shown in figure 4. No absorption in the blue region occurs upon irradiation and an isosbestic point at 268 nm is present. Moreover, no yellowing was observed in the irradiated films, indicating that a clean photoisomerization process occurs. To verify this conclusion, NMR measurements were also performed on a diluted solutions of **5** in deuterated dichloromethane. The spectral changes upon irradiation were compared with the spectra of the pure compounds, i.e. *E*-isomer **5** and the *Z*-isomer of **5,** which is **6**. The latter compound was prepared by photolysis of **5** followed by chromatographic separation

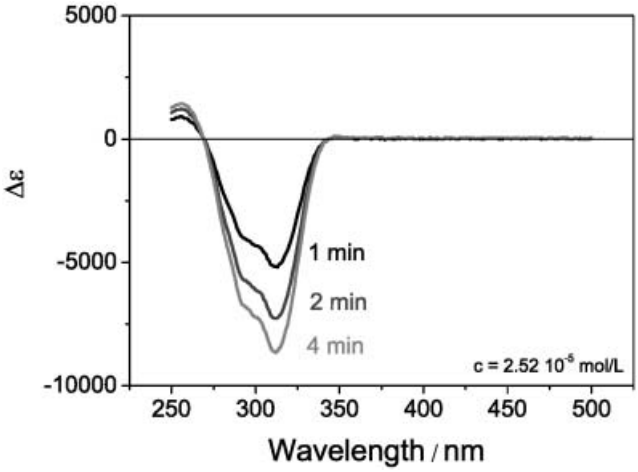

Figure 4. The difference UV-vis absorption spectra (i.e. the non-irradiated spectrum is subtracted from the irradiated one) for various irradiation times of compound **5** in acetonitrile.

of both isomers (scheme 3). It was concluded from the spectral data that in solution a clean *E–Z* photoisomerization took place. This process, in combination with the film properties and isotropization efficacy, makes compound **5** the preferred compound for making patterned retarders.

3.3. *The origin of the isotropization of nematic monomer mixtures by irradiation*

To elucidate whether the shift in transition temperature and the change in isothermal birefringence is solely attributable to the *Z*-isomer formed by photolysis, the birefringence dependence on temperature was studied on two sets of films: (1) on films prepared from **1** and **5** in a 1:1 weight ratio irradiated for various exposure times and (2) on films in which compound **5** was partially replaced by its *Z*-isomer **6** that had not been irradiated at all. Figure 5 (*a*) shows the birefringence ($\Delta n = R/d$) as a function of temperature measured on spin-coated films made from **1** and **5** in a 1:1 weight ratio that have been irradiated for various periods of time in air. No hysteresis was found, implying that no unwanted reactions, such as polymerization, took place during heating. Similar to the curves presented in figure 2 (*a*), the birefringence decreased monotonically when the temperature was raised in the nematic phase range and dropped to zero at the N-I transition. Pure liquid crystals exhibit a critical value in their order parameter (typically in the range of 0.25–0.5 [20]) at which the homogeneous nematic system transforms instantaneously into a homogeneous isotropic fluid [20–23]. However, in the monomeric systems studied in this paper, the simultaneous presence of isotropic and nematic domains — referred to as the biphasic region

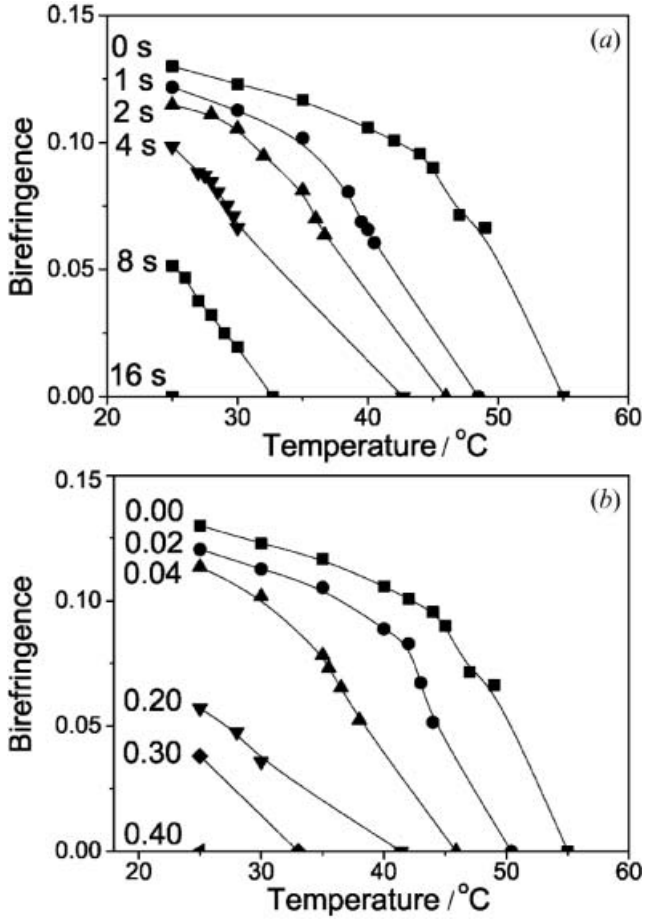

Figure 5. (*a*) The birefringence of an isomerized 1.7 µm thick film made of **1** and **5** in weight ratio 1:1 as a function of temperature for various irradiation times at an intensity of 5 W cm^{-2} using a Fairlight system. (*b*) The birefringence of a film for which the composition was varied by replacing compound **5** partially by **6.** The fraction of **6** (*x*) is indicated in the figure; the films are NOT exposed. The weight ratio of the compounds **1**, **5** and **6** was 1:(1-*x*):*x*, respectively; the film thickness was 1.7 µm.

— was observed at a temperature close to the N-I transition. The onset of the biphasic region occurred around a birefringence of about 0.08 for all films, while the width of the biphasic region increased with exposure time. The presence of the biphasic region impairs the isotropization: a relatively high temperature is required to isotropize the last nematic domains. For instance, when the film is exposed for 4 s, the onset of the biphasic region occurs at 30°C, while it takes another 13°C to completely isotropize the film. The phenomenon of the broadening of the N-I transition and the appearance of a biphasic region has been reported as a consequence of the presence of non-mesogenic compounds in nematic hosts [20, 24, 25]. Apart from the biphasic region, two other distinct features can be

observed as a function of exposure time: the N-I transition shifts incrementally to lower temperatures upon incremental exposure and, as a result, the isothermal birefringence decreases, thus allowing for isotropization at room temperature after 16 s exposure.

For comparison, we spin-coated films from mixtures containing **1**, **5** and **6**. Figure 5 (*b*) shows the determined birefringence as a function of the temperature for 1:(1–x):x mixtures of **1**, **5** and **6**, respectively (i.e. compound **5** is partially replaced by its *Z*-isomer **6**). The shape of the curves obtained for various concentrations of *Z*-isomer are similar to those obtained by irradiation, as demonstrated in figure 5 (*a*), including the occurrence of a biphasic region. When 40 % of the *E*-isomer (x=0.4) is replaced by the *Z*-isomer (i.e. the film consists of 20% *E*-isomer), an isotropic film at room temperature is obtained.

In order to verify whether the *Z*-isomer is purely accountable for the shift in the transition temperature, the conversion of irradiated films used to obtain the data set of figure 5 (*a*) was analysed by HPLC. The films were completely dissolved in the eluent and the mass injected into the column passed through it with no problems. The chromatogram showed a clear separation of the peaks and the evolution of the peak corresponding to the *Z*-isomer at the expense of the peak associated with the *E*-isomer. Figure 6 summarizes the HPLC analysis results by plotting the measured transition temperature against the *Z*-isomer ratio (x) determined with HPLC. The figure includes the transition temperature measured on films made from mixtures in which compound **5** has been partially replaced by **6**, i.e. figure 5 (*b*). The data correspond well with each other. The close resemblance of both data sets shows that the *E–Z* photoisomerization process is clean and solely accountable for the isotropization of the monomeric film.

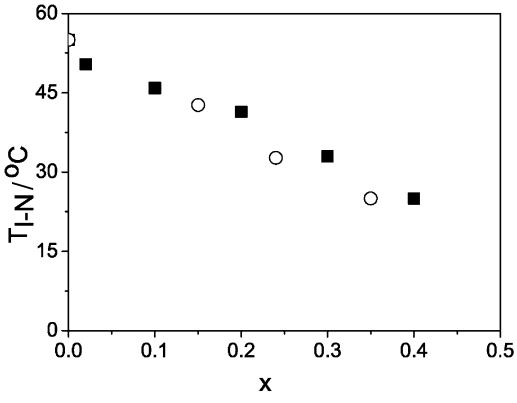

Figure 6. The nematic-to-isotropic transition temperature as a function of the fraction of **6** (x) in a mixture made of **1**, **5** and **6** in a 1:(1-x):x weight ratio obtained by mixing the three components (■) or by irradiating a 1:1 mixture of **1** and **5** and determining the amount of **6** by HPLC (○).

The main driving force of isotropization is the shift in the transition temperature beyond room temperature. A low initial transition temperature is beneficial for the isotropization process as it allows for a short exposure time, which is found to be crucial for a clean *E–Z* photoisomerization process in concentrated nematic systems; HPLC analysis of films that were exposed for longer than 60 s showed the presence of species other than those expected from the *E–Z* isomerization process in the chromatogram. These species may include oligomers due to unwanted polymerization and cycloaddition reaction products of the cinnamate derivatives **5** and **6**. These cycloaddition products are known to be formed after relatively long irradiation of concentrated mixtures of cinnamic acid derivatives [26, 27]. In addition, dissolution of the complete film was hampered considerably. This also indicates that for long exposure times unwanted polymerization has taken place.

3.4. *Patterned thin film retarders for application in transflective LCDs*

Compound **5** meets all the demands required for an optical film applied in a transflective LCD. The compound photo-reacts only in accordance with the *E–Z*-isomerization process, the orientation of the monomeric compounds in films made from **1** and **5** in a 1:1 weight ratio is planar, and isotropization of the films succeeds within 16 s without unwanted photopolymerization or yellowing. In order to verify whether these films could also be isotropized locally, we exposed the film to UV light through a mask for 16 s in air. Subsequently, the film was flood exposed to UV light in a nitrogen atmosphere to polymerize the entire film, thus freezing in the molecular order. Figure 7 illustrates schematically the process steps of the photo-patterning technology.

Figure 8 shows a microscopic image between crossed polarizers of such a patterned thin film consisting of both $1 \times 1\,\mathrm{mm}^2$ and $100 \times 100\,\mu\mathrm{m}^2$ squares. The birefringent $1 \times 1\,\mathrm{mm}^2$ domains appear bright, whereas the isotropic domains appear black. The retardation is 170 nm and 20 nm in the centre of the birefringent and isotropic domains, respectively. A homogeneous retardation within an entire domain is, however, not obtained: the interface between the birefringent and isotropic part as observed between crossed polarizers consists of a bright edge at the isotropic side and a grey edge at the birefringent side. The grey-scaling in the microscopic picture is related to the local retardation of the film: the retardation increases with brightness. The

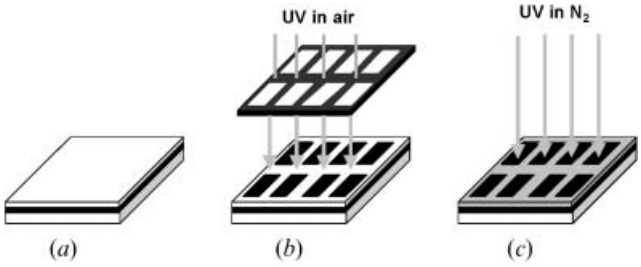

Figure 7. Schematic representation of the manufacturing process of a photo-patterned retardation film comprising birefringent and isotropic domains. (*a*) The retarder mixture is spin-coated on top of a substrate with an alignment layer. (*b*) The film consisting of monomers in their nematic phase (white) is lithographically isomerized in air to create the isotropic domains (black). (*c*) The entire film is subsequently polymerized by a flood exposure in a nitrogen atmosphere to fix both the birefringent (grey) and isotropic domains.

retardation, in turn, depends on the product of the birefringence and film thickness. Examination of the surface profile of the patterned thin film revealed a complicated corrugated surface, as shown in figure 9 (*a*). The arrow in figure 8 indicates the scan position of the surface profile. The birefringent part is about 500 nm higher than the isotropic part, while a protrusion of 1200 nm is present at the isotropic side, causing the bright interface in figure 8 (*a*). Accordingly, an indentation is present in the birefringent domain that enforces the grey scale at the interface with the isotropic domain. The surface corrugation is presumably the result of lithographic exposure of monomers, which is known to induce mass transport to the exposed areas. This phenomenon is used for the fabrication of diffusers [28, 29] or to create diffractive elements [30], but is highly undesirable in the fabrication of patterned thin film retarders [11]. For isotropic acrylate systems that are lithographically exposed

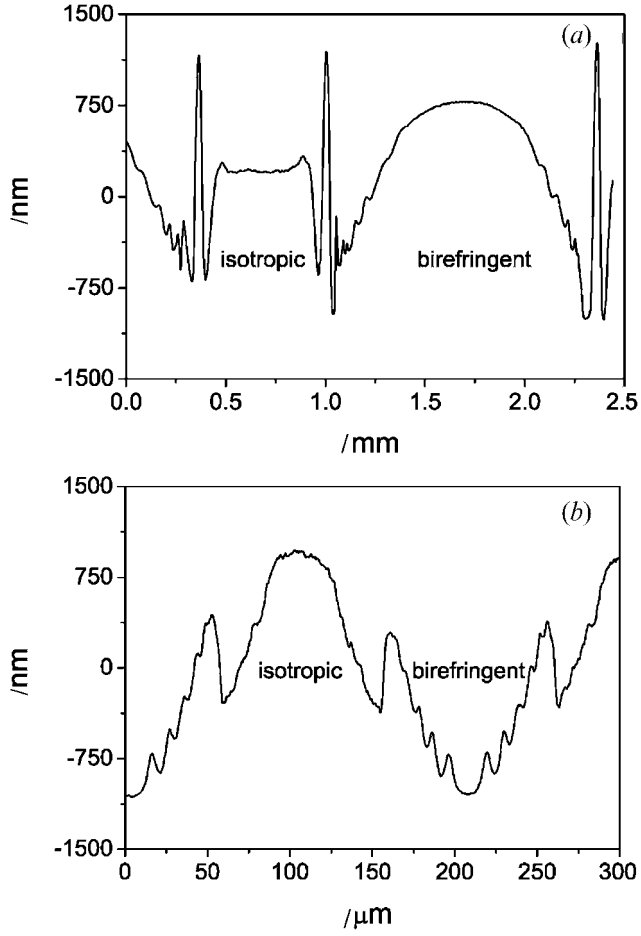

Figure 9. Surface profiles of the $1 \times 1\,\mathrm{mm}^2$ (*a*) and $100 \times 100\,\mu\mathrm{m}^2$ (*b*) squares of a photo-patterned and photopolymerized thin film measured by interferometry.

to induce photopolymerization, the mass transport phenomena have been described by monomer diffusion to the exposed areas and could be modelled in terms of

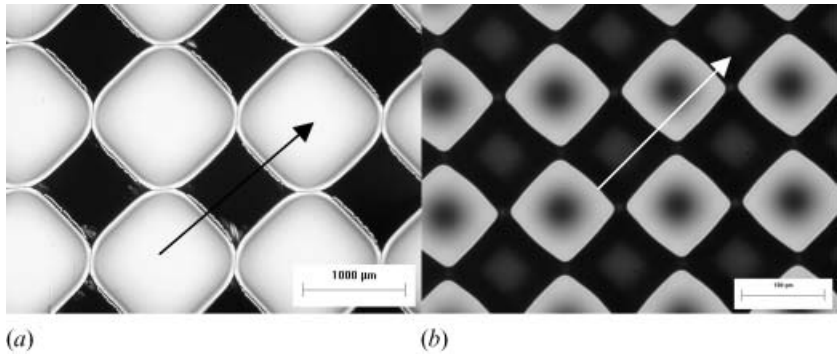

Figure 8. Polarization microscopy images of photo-patterned optical films. The orientation of the director in the nematic domain (bright) is 45° with respect to the transmissive axes of the crossed polarizers. The dark domains are isomerized and subsequently polymerized in the isotropic state. The bright areas are photopolymerized in the nematic state. (*a*) $1 \times 1\,\mathrm{mm}^2$, (*b*) $100 \times 100\,\mu\mathrm{m}^2$.

chemical potential of the reacting and the formed species. In this case, mass transport is induced by isomerization and not polymerization. The formation of the *Z*-isomer is seemingly sufficient to create a driving force for mass transport during the lithographic *E–Z* isomerization process. However, so far we have not elucidated the origins for mass transport induced by lithographic *E–Z*-isomerization.

Figures 8 (*b*) and 9 (*b*) present a microscopic image between crossed polarizers and the surface profile of a $100 \times 100\,\mu m^2$ patterned thin film, respectively. The microscopic image reveals a brighter area in the centre of the isotropic domain and a darker area in the centre of the birefringent domain. These grey scales can also be explained by surface corrugation in accordance with the $1 \times 1\,mm^2$ domains. Figure 9 (*b*) distinctly shows that the centre of the isotropic domain is about 2 μm thicker than the centre of the birefringent domain. This represents an extreme difference in thickness, given the initial film thickness of 1.7 μm. Hence, the isotropic domain has become thicker at the expense of the film thickness of the birefringent domain. As a result, the retardation in the birefringent domain has become very small, i.e. 70 nm instead of 170 nm, which gives it a greyish appearance. The origin of the brighter appearance of the centre in the isotropic part is presumably related to the mass transport of the monomers to the exposed areas. Due to this mass transport, the composition of the monomeric film changes. As a consequence, the transition temperature of the monomeric mixture increased again, resulting in a small birefringence. A complete isotropic domain was obtained at prolonged irradiation. However, a prolonged irradiation allows for more mass transport, which resulted in a birefringent domain with a retardation value close to zero [11]. With regard to the application of these patterned thin films as a retarder in transflective LCDs, the mass transport of monomers should be reduced; this may be achieved by carefully matching the monomer size, crosslinking degree, surface tension and reactivity [31, 32].

4. Conclusions

Isomerizable diacrylates derived from cinnamic acid have been designed and synthesized with the aim of making films with alternating isotropic and birefringent domains by applying the *E–Z* isomerization process at room temperature. A suitable compound is compound **5** derived from cyclohexyl cinnamate, which has a low transition temperature. This compound does not show yellowing upon irradiation, unlike phenyl cinnamate derivatives. The orientation of the monomeric liquid crystalline diacrylates in films spin-coated from a xylene solution containing **5** and nematic diacrylate **1** in a 1:1 weight ratio is uniaxial and planar. Isotropization of the film is achieved within 16 s exposure using $5\,mW\,cm^{-2}$ 313 nm UV light. It is shown that a shift in transition temperature enforces the isotropization of the birefringent film and that for short irradiation times this shift in transition temperature is attributed solely to the *E–Z* isomerization process. The molecular order of the monomers is changed locally with a resolution of up to $100 \times 100\,\mu m^2$ to form thin films with alternating birefringent and isotropic parts by using a combination of photoisomerization in air and photopolymerization in a nitrogen atmosphere.

Acknowledgements

We would like to thank Mr G.L.T.van den Heuvel of Philips Research for performing the HPLC experiments.

References

[1] B.M.I. van der Zande, S.J. Roosendaal, C. Doornkamp, J. Steenbakkers, J. Lub. *Adv. funct. Mat.* (in the press).
[2] S.J. Roosendaal, B.M.I. van der Zande, A.C. Nieuwkerk, C.A. Renders, J.T.M. Osenga, C. Doornkamp, E. Peeters, J. Bruinink, J.A.M.M. van Haaren. *SID Dig. tech. Pap.*, pp. 78–81, (2003).
[3] C. Doornkamp, B.M.I. van der Zande, S.J. Roosendaal, L.W.G. Stofmeel, J.J. van Glabbeek, J.T.M. Osenga, J.A.M. Steenbakkers. *Proc. IDW'03*, pp. 685–688 (2003).
[4] M. Schadt, H. Seiberle, A. Schuster, S.M. Kelly. *J. appl. Phys.*, **34**, 3240 (1995).
[5] A. Bobrovsky, N. Boiko, V. Shibaev, J. Stumpe. *J. Photochem. Photobiol. A, Chem.*, **163**, 347 (2004).
[6] T. Fisher, L. Läsker, J. Stumpe, S. Kostromin. *J. Photochem. Photobiol. A, Chem.*, **80**, 453 (1994).
[7] D.J. Broer. *Radiation Curing in Polymer Science and Technology,* Vol. 3, Chap. 12, J.P. Fouassier, J.F. Rabek (Eds). Elsevier (1993).
[8] B.M.I. van der Zande, A.C. Nieuwkerk, M. van Deurzen, C.A. Renders, E. Peeters, S.J. Roosendaal. *SID Dig. tech. Pap.*, pp. 194–197 (2003).
[9] S.J. Park, C.G. Jhun, K.-H. Park, J.C. Kim, T.-H. Yoon. *Proc. IDW'03*, pp. 159–162 (2003).
[10] B.M.I. van der Zande, C. Doornkamp, S.J. Roosendaal, J. Steenbakkers, A. Op t Hoog, J.T.M. Osenga, J.J. van Glabbeek, L. Stofmeel, J. Lub, M. Shibazaki, K. Asahara, T. Inada, M. Yoshiga, S. Kawata. *J. Soc. Inf. Displ.*, **13**, 627 (2005).
[11] B.M.I. van der Zande, J. Lub, C.M. Leewis, J. Steenbakkers, D.J. Broer. *J. appl. Phys.*, **97**, 123519–1 (2005).
[12] J. Lub, W.P.M. Nijssen, R.T. Wegh, J.P.A. Vogels, A. Ferrer. *Adv. func. Mat.*, **15**, 1961 (2005).
[13] J. Lub, W.P.M. Nijssen, R.T. Wegh, I. De Francisco, M.P. Ezquerro, B. Malo. *Liq. Cryst.*, **32**, 1031 (2005).
[14] S. Singh, D. Creed, C.E. Hoyle. *Proc. SPIE*, **1774**, 2 (1993).
[15] J. Lub, J.H. van der Veen, D.J. Broer, R.A.M. Hikmet. *Macrom. Synth.*, **12**, C.K. Ober, L.J. Mathias (Eds), pp. 101–108 (2002).

[16] J. Lub, J.H. van der Veen, W. ten Hoeve. *Recl. Trav. Chim. Pays-Bas*, **115**, 321 (1996).
[17] H. Schmid. *Monatsh. Chem.*, **32**, 437 (1911).
[18] J. Lub, D.J. Broer, M.E. Martinez Antonio, G.N. Mol. *Liq. Cryst.*, **24**, 375 (1998).
[19] J. Stumpe, C. Selbmann, D. Kreysig. *J. Photochem. Photobiol.*, **58** (1991).
[20] S. Singh. *Phys. Rep.*, **324**, 107 (2000).
[21] P.G. de Gennes. *Phys. Lett. A*, **30**, 454 (1969).
[22] W. Maier, A. Saupe. *Z. Naturforsch.*, **14a**, 882 (1959); W. Moier, A. Saupe. *Z. Naturforsch*., **15a**, 287 (1960).
[23] L. Onsager. *Ann. N.Y. Acad. Sci.*, **51**, 627 (1949).
[24] G.A. Oweimreen, D.E. Martire. *J. chem. Phys.*, **72**, 2500 (1980).
[25] P.K. Mukherjee. *Mod. Phys. Lett.*, **B 11**, 107 (1997).
[26] G. Kaup. In *Organic Photochemistry and Photobiology*, M. Horspool, P.S. Song (Eds). Chap. 3, CRC press, New York (1995).
[27] M. D'Auria, A. Vantaggi. *Tetrahedron*, **48**, 2523 (1992).
[28] C. de Witz, D.J. Broer. *Polym. Prepr. Am. chem. Soc. Div. polym. Chem.*, **44**, 236 (2003).
[29] M. Ibn-Elhaj, M. Schadt. *Nature*, **410**, 796 (2001).
[30] P. Kossyrev, M.E. Sousa, G. Crawford. *Adv. funct. Mater.*, **14**, 1227 (2004).
[31] C.M. Leewis, P.H.A. Mutsaers, A.M. de Jong, L.J. van IJzendoorn, M.J.A. de Voigt, M.Q. Ren, F. Watt, D.J. Broer. *J. chem. Phys.*, **120**, 1820 (2004).
[32] C.M. Leewis, P.H.A. Mutsaers, A.M. de Jong, L.J. van IJzendoorn, D.J. Broer, M.J.A. de Voigt. *Nucl. Instr. Meth. B*, **181**, 367 (2001).